Method for mean-line design and performance prediction of one-stage axial turbines

Lasse B. Anderson [a,*], Roberto Agromayor [a], Lars O. Nord [a]

[a] *NTNU - Norwegian University of Science and Technology, Department of Energy and Process Engineering, Trondheim, Norway*

[*] *lasse.b.anderson@ntnu.no*

Abstract

Today, expanders for Organic Rankine Cycles (ORC) are either inefficient or expensive. One reason for this is that expanders of power conversion systems usually operate under different conditions over an annual perspective. Still, they are designed to perform best at a single operating point. In view of this limitation, it is suggested that the overall expander performance can be improved by taking into account off-design operation in the design process. As the first step in this direction, this paper presents a two-fold method for design optimization and performance analysis of one-stage axial turbines. The method utilizes the same mean-line model for performance analysis and design optimization, ensuring consistency between the two modes. In addition, the proposed method evaluates the turbine performance at three stations for each blade row: inlet, throat and exit, and employs a novel numerical treatment of flow choking that automatically determines which blade rows are choked as part of the solution. Furthermore, the method was validated against cold-air experimental data from three different one-stage axial turbines, at both on- and off-design conditions. The model predicts design point efficiencies between 1.1 and 4.5 percentage points off the experimental values. The model was also able to capture the trend of mass flow rate as a function of total-to-static pressure ratio and angular speed. However, an unphysical behavior was observed as the pressure ratio approaches the critical value, and further developments of the model are required. It is envisioned that the proposed method will serve as foundation for a robust design methodology that will enable higher expander performance over a range of operating conditions.

1. Introduction

The Rankine Cycle technology is used to convert heat from external sources into electrical power, making it suitable to exploit low-carbon energy sources such as geothermal reservoirs, concentrated solar radiation and waste heat from industrial processes (Colonna et al. 2015). The Rankine cycle in its simplest form consist of four elements: condenser, pump, evaporator and expander (Figure 1). Electrical power is generated as the working fluid flows through the expander, and produces a torque on a shaft coupled to an electrical generator. After the expander, the working fluid is condensed, pressurized through the pump and heated before it enters the expander once again. When the heat source temperature is limited, it becomes beneficial to utilize organic compound as working fluid, to avoid condensation within the expander, and the cycle is referred to as Organic Rankine Cycle (ORC).

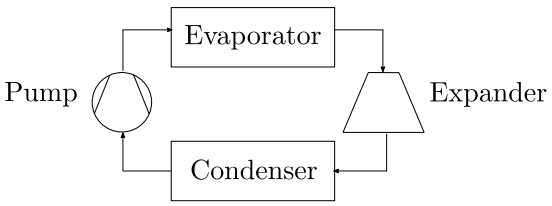

Figure 1: Simple ORC configuration.

Furthermore, adopting an organic fluid in the Rankine cycle paves the way towards compact and cost-efficient turbo-expanders. The higher molecular weight of these fluids leads to a lower enthalpy drop compared to conventional steam cycles (Macchi and Astolfi 2017). This enables turbo-expanders with a low number of stages, and operation at relatively low rotational speed. However, the expansion ratio for each stage is usually very high in compact ORC turbines, and combined with a low speed of sound this often leads to transonic or even supersonic flows. In addition, non-ideal gas effects could be prominent as the expansion process usually occurs in the dense vapor region. These effects combined result in additional losses and non-conventional turbine designs, where traditional design methods are insufficient (Persico and Pini 2017).

The first step of the design process for ORC turbines is to decide which type of architecture to use. This could be axial turbine, radial turbine or a hybrid solution. This choice is usually based on statistical data or overall machine correlations (Macchi and Astolfi 2017). The next step is the preliminary design phase. The purpose of this phase is to subdivide the the expansion process between turbine stages, thus specifying the thermodynamic and kinetic state at inlet and exit for each cascade. For this reason, the preliminary design is crucial for the whole design process. Furthermore, this phase makes use of mean-line models, which assume that the flow is uniform in the circumferential and spanwise directions (Denton 1993). Inlet and exit conditions for each cascade are determined

by solving the mass, momentum and energy conservation equations along with an equation of state. In addition, the mean line approach requires empirical correlations to estimate entropy generation throughout the turbine, referred to as loss models. The turbine performance is predicted with the mean-line model, given a geometry and a set of thermodynamic boundary conditions for the turbine. Thus, the preliminary design can be accomplished combining the mean-line model with an optimization routine that finds the best geometry that optimizes an objective function, commonly being the isentropic efficiency (Persico and Pini 2017).

In most cases, the turbine design process only takes into account the performance at one operation point (i.e., the design point). However, ORC power systems are frequently connected to heat sources and sinks with variable load. Heating and cooling duties from sources such as exhaust from gas turbines or cooling by ambient air are very likely to vary, and this will propagate to change expander conditions (Jiménez-Arreola et al. 2018; Macchi and Astolfi 2017). In order to improve efficiency of ORC expanders it is therefore suggested that the design process should account for variable expander conditions. In other words, rather than designing an expander for one single design point, the expander is designed considering a range of operating conditions. This multipoint optimization strategy has been adopted in several high-fidelity design methods, and shows great promise to rise the efficiency of the turbine at off-design conditions (Aissa et al. 2019; Bonaiuti and Zangeneh 2009; Châtel, Verstraete, and Coussement 2020; M. Pini, G. Persico, and Dossena 2014; Sanchez Torreguitart, Verstraete, and Mueller 2018). However, to the authors' knowledge, the use of multipoint optimization strategies for preliminary turbine design has not been considered yet.

The objective in this paper is to formulate a two-fold method for the design optimization and performance analysis of one-stage axial turbines. The method uses the same mathematical model for performance analysis and design optimization, and both modes are formulated as nonlinear programming problems, which are solved using gradient-based optimization algorithms. The mathematical model follows a mean-line approach and, in contrast to most of the methods available in the open literature, evaluates the turbine performance at three stations for each blade row: inlet, throat and exit, making it suitable for choked flow conditions. The model is validated against numerical cases from the literature and experimental data, at both on- and off-design conditions. It is envisaged that the methods presented herein will serve as building blocks to develop a robust design methodology for axial turbines that will enable higher performance over a range of operating conditions.

The outline is as follows: the next section describes the mathematical model used for the two-fold method, followed by a section on the differences of the two modes. The model validation is then given before a design case study is presented. At last, the content is summarized before suggestions for further work are made.

2. Mathematical model

This section describes a mathematical model for assessment of one-stage axial turbines. This model is used for both performance analysis and preliminary design of one-stage axial turbines. The variables used to define the turbine geometry are presented first, followed by modelling

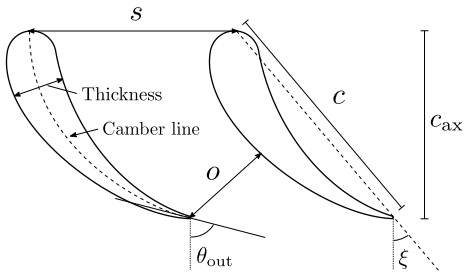

Figure 2: Geometry of the cross-sectional shape of the blades.

of velocity triangles, thermodynamic properties and loss prediction. The mathematical model presented here is based on the work of Agromayor and Nord, who proposed a method for the design optimization of axial turbines (Agromayor and Nord 2019). However, the objective here is to extend the method and include performance analysis in addition to design optimization, leading to certain model differences. Notably, the mass flow rate is computed, rather than being an input variable, because the performance analysis should predict the mass flow rate. Furthermore, thermophysical properties and velocity triangles are assessed at the throat, in addition to the inlet and exit of each cascade, to predict choked flow. Consequently, the set of input variables will deviate from the the work of Agromayor and Nord.

The model is implemented in the Python programming language and is released under an open source license. This does not only increase the transparency and reproducibility of the results, but also enables other researchers and industry practitioners to use the code for their needs or contribute to its development.

2.1. Turbine geometry

The geometrical variables considered in the mean-line turbine model include parameters related to the cross-sectional shape of the blades, distance between adjacent blades and extent in radial direction. Figure 2 illustrates the geometrical variables related to the cross sectional shape of the blades. The chord c is the distance between leading and trailing edge, while the camberline is the line halfway between pressure and suction surfaces of the blade. Axial chord c_{ax} is the axial component of the chord. The blade thickness is the distance between pressure and suction surfaces, perpendicular to the camber. Furthermore, the metal angle θ is defined as the angle between axial direction and tangential component of the camber line. The pitch s is the distance between two adjacent blades, and the opening o is the distance between the trailing edge to the suction surface of the adjacent blade, measured normal to the outlet metal angle. The stagger ξ is the angle between axial direction and chord line. Maximum thickness t_{max} and trailing edge thickness t_{te} must also be considered for loss prediction (Kacker and Okapuu 1982).

In addition, the parameters describing the shape of the blade in radial direction are also included in the model, such as mean radius r_m, blade height H and tip-clearance gap t_{cl} (see Figure 3). The blade height may vary from inlet to outlet of the blade cascade, and the flaring angle δ_{fl} describes this variation.

In order to reduce the number of input variables, some relations between geometrical variables are used. The first

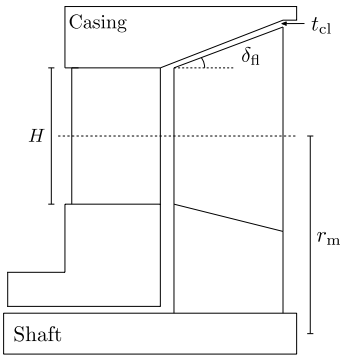

Figure 3: Geometry of turbine blades in radial direction.

relation is the cosine rule, which relates the blade opening with the exit metal angle (Saravanamutto et al. 2017):

$$o \approx s \cdot \cos(\theta_{\mathrm{out}}) \tag{1}$$

Furthermore, Kacker and Okapuu proposed a formula to approximate the maximum thickness to chord ratio as a function of the blade camber angle ($\Delta\theta = |\theta_{\mathrm{in}} - \theta_{\mathrm{out}}|$) (Kacker and Okapuu 1982):

$$\frac{t_{\max}}{c} = \begin{cases} 0.15, \Delta\theta \leq 40^\circ \\ 0.15 + 1.25 \cdot 10^{-3} \cdot (\Delta\theta - 40) \\ 0.25, 120^\circ \leq \Delta\theta \end{cases} \tag{2}$$

If one assumes that the camber line is a circular arc, the stagger angle is given by (Dixon 2014):

$$\xi = \frac{1}{2}(\theta_{\mathrm{in}} + \theta_{\mathrm{out}}) \tag{3}$$

Using the definition of stagger angle, the axial chord can be determined from the chord:

$$c_{\mathrm{ax}} = c \cdot \cos(\xi) \tag{4}$$

The mean radius is assumed to be constant, meaning the blade converge/diverge equally at the inner and outer wall of the flow passage, then the stator inlet and exit blade heights are determined by the mean blade height and stator flaring angle:

$$H_{\mathrm{in,s}} = H_{\mathrm{s}} - \tan(\delta_{\mathrm{fl,s}}) \cdot c_{\mathrm{ax,s}} \tag{5}$$

$$H_{\mathrm{out,s}} = H_{\mathrm{s}} + \tan(\delta_{\mathrm{fl,s}}) \cdot c_{\mathrm{ax,s}} \tag{6}$$

Furthermore, the blade height at stator exit is assumed to be equal to rotor inlet, meaning no flaring between blade rows. Consequently, for rotor row, the flaring angle is determined from inlet and mean blade height, which further gives the exit blade height:

$$\delta_{\mathrm{fl,r}} = \arctan(\frac{H_{\mathrm{r}} - H_{\mathrm{out,s}}}{c_{\mathrm{ax,r}}}) \tag{7}$$

$$H_{\mathrm{out,r}} = H_{\mathrm{r}} + \tan(\delta_{\mathrm{fl,r}}) \cdot c_{\mathrm{ax,r}} \tag{8}$$

Another parameter needed for loss calculations is the hub-to-tip ratio:

$$r_{\mathrm{ht}} = \frac{r_{\mathrm{h}}}{r_{\mathrm{t}}} = \frac{r_{\mathrm{m}} - H/2}{r_{\mathrm{m}} + H/2} \tag{9}$$

At last, the area at inlet, exit and throat of each blade row is calculated by the following equations:

$$A_{\mathrm{in}} = 2\pi \cdot r_{\mathrm{m}} \cdot H_{\mathrm{in}} \tag{10}$$

$$A_{\mathrm{out}} = 2\pi \cdot r_{\mathrm{m}} \cdot H_{\mathrm{out}} \tag{11}$$

$$A_{\mathrm{throat}} = 2\pi \cdot r_{\mathrm{m}} \cdot H_{\mathrm{throat}} \cdot \cos(\theta_{\mathrm{out}}) \tag{12}$$

Table 1: Geometrical variables of the axial turbine.

Variable	Stator	Rotor
Mean radius	r_{m}	
Blade height	H_{s}	H_{r}
Aspect ratio	$(H/c)_{\mathrm{s}}$	$(H/c)_{\mathrm{r}}$
Pitch to chord ratio	$(s/c)_{\mathrm{s}}$	$(s/c)_{\mathrm{r}}$
TE thickness to opening ratio	$(t_{te}/o)_{\mathrm{s}}$	$(t_{te}/o)_{\mathrm{r}}$
Inlet metal angle	-	$\theta_{\mathrm{in,r}}$
Outlet metal angle	$\theta_{\mathrm{out,s}}$	$\theta_{\mathrm{out,r}}$
Flaring angle	$\delta_{\mathrm{fl,s}}$	-
Tip clearance	-	t_{cl}

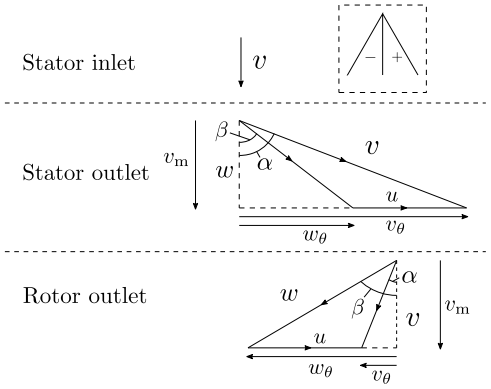

Figure 4: Velocity triangles. Sign convention for the angles is illustrated in the upper right corner.

In total, the geometry of the stage is defined using fourteen variables. The geometrical variables are listed in Table 1 and are inputs to the model.

2.2. Velocity triangles

The velocity triangles (Figure 4) are evaluated at each station of the turbine, and are calculated with the following equations:

$$\begin{aligned} v_{\mathrm{m}} &= v \cdot \cos(\alpha) \\ v_\theta &= v \cdot \sin(\alpha) \\ w_{\mathrm{m}} &= w \cdot \cos(\beta) \\ w_\theta &= w \cdot \sin(\beta) \\ w_\theta &= v_\theta - u \end{aligned} \tag{13}$$

Where the blade velocity u is calculated from the mean radius and the rotational speed Ω:

$$u = \Omega \cdot r_{\mathrm{m}} \tag{14}$$

The stator inlet flow angle is fixed to zero, while the flow angles at throats are assumed to equal the exit metal angles, which imply zero deviation:

$$\beta_{\mathrm{throat}} = \theta_{\mathrm{out}} + \delta \approx \theta_{\mathrm{out}} \tag{15}$$

Thus, the velocity at each station, exit flow angles and rotational speed are input variables. These are listed in Table 2, except for the rotational speed, which is treated similarly as the geometrical variables (see Section 3).

Table 2: Velocity, flow angles and static pressure variables that are inputs for the model.

Variable	Symbol
Stator inlet velocity	$v_{\mathrm{in,s}}$
Stator throat velocity	$v_{\mathrm{throat,s}}$
Stator exit velocity	$v_{\mathrm{out,s}}$
Rotor throat relative velocity	$w_{\mathrm{throat,r}}$
Rotor exit relative velocity	$w_{\mathrm{out,r}}$
Stator exit absolute flow angle	$\alpha_{\mathrm{out,s}}$
Rotor exit relative flow angle	$\beta_{\mathrm{out,r}}$
Stator throat static pressure	$p_{\mathrm{throat,s}}$
Stator exit static pressure	$p_{\mathrm{out,s}}$
Rotor throat static pressure	$p_{\mathrm{throat,r}}$

Table 3: Thermodynamic boundaries for the turbine.

Variable	Symbol
Working fluid	-
Inlet stagnation temperature	$T_{0,\mathrm{in}}$
Inlet stagnation pressure	$p_{0,\mathrm{in}}$
Outlet static pressure	p_{out}

2.3. Thermodynamics

The thermodynamic boundaries for the turbine model must also be specified. These variables are usually obtained from a system-level analysis of the power cycle and include states at inlet and outlet of the turbine, as well as the working fluid. These variables are listed in Table 3.

In addition to these input variables, other thermophysical variables need to be evaluated through the turbine stage. Similarly as for the velocity triangles, these are assessed at each station of the turbine. For simple compressible systems, the state is completely specified for two independent intensive properties (Moran et al. 2015). A library of thermophysical properties is required for these calculations, and in this method CoolProp is used (Bell et al. 2014). Since the stagnation state is prescribed at the turbine inlet, entropy and enthalpy are used to calculate thermophysical properties at this station:

$$[\rho, a, p, \mu]_{\mathrm{in}} = f(s_{\mathrm{in}}, h_{\mathrm{in}}) \tag{16}$$

where ρ is the fluid density, a speed of sound, and μ is the dynamic viscosity. Through the rest of the turbine, static pressure and enthalpy are used to determine the dependent thermophysical properties. This means static pressure at stator throat, between blade rows and rotor throat must be provided as input (see Table 2). This was found to be more robust than using entropy and enthalpy as input variables.

$$[\rho, a, s, \mu] = f(p, h) \tag{17}$$

The enthalpy at each station of the turbine is calculated by the conservation of rothalpy:

$$h + \frac{1}{2}w^2 - \frac{1}{2}u^2 = \mathrm{constant} \tag{18}$$

Through the stator row this is reduced to conservation of stagnation enthalpy:

$$h_{0,\mathrm{s}} = \mathrm{constant} \tag{19}$$

With the velocity triangles and thermophysical properties, the mass flow rate, Mach and Reynolds number may be evaluated:

$$\dot{m} = \rho v A \tag{20}$$

$$\mathrm{Ma} = \frac{v}{a} \tag{21}$$

$$\mathrm{Re} = \frac{\rho V c}{\mu} \tag{22}$$

2.4. Loss model

What is left is to predict the entropy generation in the turbine. For this purpose, a loss coefficient must be defined, and a loss model to predict this loss coefficient must be selected. In this work, the Kacker and Okapuu loss model is adopted for its maturity and accuracy (Kacker and Okapuu 1982), but the loss model may easily be switched to another if desired. The loss coefficient may be defined in several ways (Denton 1993), but is here formulated as the total pressure loss between inlet and exit of a blade row, divided by the exit dynamic pressure:

$$Y_{\mathrm{definition}} = \frac{p_{0,\mathrm{rel,in}} - p_{0,\mathrm{rel,out}}}{p_{0,\mathrm{rel,out}} - p_{\mathrm{out}}} \tag{23}$$

This is referred to as the total pressure loss coefficient, and it is adopted because the Kacker and Okapuu loss model is based on this definition. The deviation between the total pressure loss coefficient computed from its definition and the value determined by the loss model must be assessed:

$$Y_{\mathrm{error}} = Y_{\mathrm{definition}} - Y_{\mathrm{lossmodel}} \tag{24}$$

This error should be zero, and the states through the turbine must be such that this is satisfied. This is discussed further in Section 2.5 and 3. Furthermore, the loss coefficient is here assessed at both throat and exit for each blade row. The loss model itself is formulated to predict losses between inlet and exit of a blade row and not between inlet and throat. However, the alternative is to assume isentropic flow between inlet and throat, but it was observed that this strategy predicted losses less accurately compared to the original formulation. A logical explanation behind this is that the state at the throat is more likely to be similar to the exit rather then the inlet.

2.5. Closing of equations

With the use of the equations above, the mass flow rate, loss coefficient and Mach number can be evaluated at each station using the variables in Tables 2 and 3. However, by only using the equations above, the mass flow rates at each station are not necessarily equal, the Mach number at the throat is not necessarily maximum one and the error between the loss model coefficient and loss coefficient obtained from its definition is not necessarily zero. This forms a set of equations that must be satisfied for each blade row in order for the flow to be physically feasible:

$$\begin{aligned} \dot{m}_{\mathrm{in}} - \dot{m}_{\mathrm{throat}} &= 0 \\ \dot{m}_{\mathrm{in}} - \dot{m}_{\mathrm{out}} &= 0 \\ \mathrm{Ma}_{\mathrm{throat,rel}} - \min(1, \mathrm{Ma}_{\mathrm{out,rel}}) &= 0 \\ (Y_{\mathrm{def}} - Y_{\mathrm{loss}})_{\mathrm{throat}} &= 0 \\ (Y_{\mathrm{def}} - Y_{\mathrm{loss}})_{\mathrm{out}} &= 0 \end{aligned} \tag{25}$$

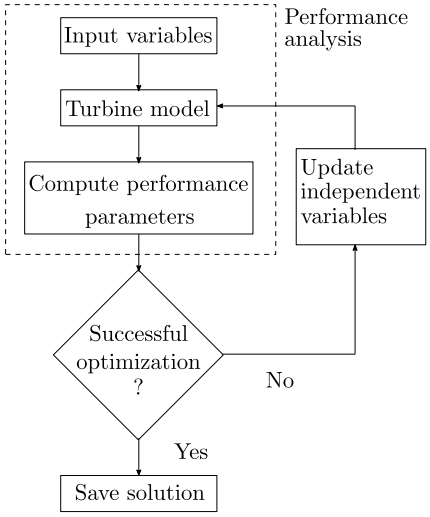

Figure 5: Workflow for the preliminary design objective and performance analysis.

In other words, this is a set of ten equations on the form $\vec{F}(\vec{x}) = 0$, where $\vec{x}$ is a vector with the ten variables in Table 2. The thermophysical states and velocity triangles can be determined by ensuring that Eq. (25) is satisfied. The strategy to ensure this is different for the two modes of the two-fold method, and are presented in the next section.

3. Optimization vs. performance analysis

The model described above is used for two purposes: preliminary design and performance analysis of one-stage axial turbines. Figure 5 presents the workflow for the preliminary design mode, and where the performance analysis fits into this. The turbine model is used for both preliminary design and performance analysis to ensure consistency between the two modes, but there are certain differences in problem formulation, which will be described in this section.

3.1. Optimization

The goal of the optimization objective is to find the optimal geometry given the thermodynamic fixed variables. In this case, the thermodynamic boundaries (Table 3) are fixed parameters, while the geometry, rotational speed and input velocity/static pressure (Tables 1 and 2) are independent variables. This mode makes use of an optimization algorithm to tune the independent variables such that the optimal value of the objective function is reached while a set of bounds and constraints are respected. The optimization algorithm used in this method is the sequential quadratic programming (SQP) algorithm, available in the Scipy library (Virtanen et al. 2020). The objective function is defined as the total-to-static efficiency (Eq. (26)), but may easily be changed to other performance related parameters such as total-to-total efficiency or work output. The closing equations (Eq. (25)) are specified as a set of equality constraints to ensure a physical solution, while bounds may be defined for all independent variables. Other constraints may be added, both equality and inequality. For example, if the user desires to treat mass flow rate as an input variable, it can be imposed with an equality constraint.

$$\eta_{\mathrm{ts}} = \frac{h_{0,\mathrm{in}} - h_{0,\mathrm{out}}}{h_{0,\mathrm{in}} - h_{0,\mathrm{is}}} \tag{26}$$

Table 4: Operating conditions and comparison of performance parameters between the numerical design reference (Agromayor and Nord 2019) and model presented in this paper.

Variable	Agromayor and Nord 2019	Present work
Fluid	R125	-
$T_{0,\mathrm{in}}$	428.15 K	-
$p_{0,\mathrm{in}}$	36.18 bar	-
p_{out}	15.34 bar	-
Ω	34 738.2	-
η_{ts}	88.72%	88.44%
$\dot{m}$	11.90 kg/s	11.85 kg/s
$\dot{W}$	227.76 kW	226.12 kW

3.2. Performance analysis

The goal of the performance analysis is to assess the thermodynamic and kinetic variables given a geometry, rotational speed and thermodynamic boundaries. This means that the thermodynamic, geometrical variables (Tables 3 and 1) and rotational speed are fixed parameters, while the velocity and static pressure inputs (Table 2) are unknown variables. The unknown variables are determined by solving the system of equations from section 2.5 (Eq. (25)), with a root finder method from the Scipy library (Virtanen et al. 2020).

4. Model validation

The turbine model has been used to simulate the performance of three experimentally investigated turbines, in addition to one numerical test case. The numerical case corresponds to the case considered in (Agromayor and Nord 2019), and present work is validated against this case due to the similarities of the models. The three experimental cases are cold-air tests of one-stage axial turbines, both at subsonic and transonic conditions (Haas and Kofskey 1975; Moffitt et al. 1980; Nusbaum and Kofskey 1972). The experimental values where attempted to be replicated at design pressure ratio and design rotational speed. The metal angles were assumed to equal the design flow angles (Eq. (15)). Note that the values in the experimental reports are given in terms of equivalent conditions, and are here converted to ordinary values, using the conditions at standard sea-level (temperature: 288.15 K; pressure: 1.01325 bar).

4.1. Numerical case

The operating conditions, and corresponding performance parameters are presented in Table 4. Note that the reference case includes a diffuser model after turbine exit, which is not considered here, and the efficiency is determined with the state at the exit of the turbine. As expected the results match well as the models used in the reference case and this work are similar.

4.2. Experimental case 1

The first experimental case to be simulated is the turbine documented in (Nusbaum and Kofskey 1972). Table 5 show the operating conditions and corresponding performance parameters at design pressure ratio and rotational speed. The results show a deviation in total-to-static efficiency of 3.52 percentage points, which is larger than

Table 5: Operating conditions and comparison of performance parameters between the first experimental reference (Nusbaum and Kofskey 1972) and model presented in this paper.

Variable	Nusbaum and Kofskey 1972	Present work
Fluid	Air	-
$T_{0,\mathrm{in}}$	295.6 K	-
$p_{0,\mathrm{in}}$	13.8 bar	-
$p_{0,\mathrm{in}}/p_{\mathrm{out}}$	2.298	-
Ω	15533	-
η_{ts}	80.00%	76.48%
$\dot{m}$	2.696 kg/s	2.740 kg/s
$\dot{W}$	134.14 kW	131.58 kW

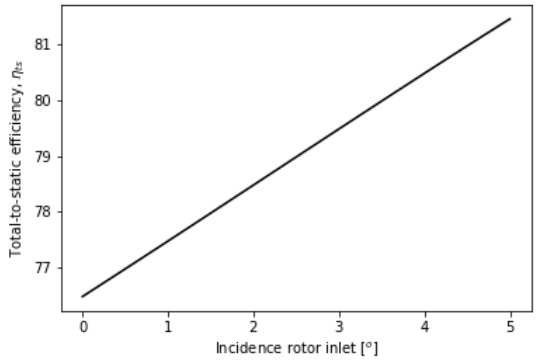

Figure 6: Total-to-static efficiency as a function of rotor inlet incidence. The relation looks linear, but it is observed that it becomes nonlinear outside this region.

the uncertainty of the loss model by Kacker and Okapuu (± 1.5 percentage points) (Kacker and Okapuu 1982). The predicted mass flow rate exceed the experimental value with 1.64%, while the predicted work out is 1.91% less than the actual value. The deviation in predicted design-point efficiency was unexpected as Agromayor and Nord used the same loss model and same reference case for validation, but predicted an efficiency within the loss model uncertainty (78.85%). Nevertheless, the report explains that the rotor inlet whirl is greater than design, and hence the assumption from Eq. (15) is not satisfied. Therefore, simulations with incidence were performed and Figure 6 shows the total-to-static efficiency as a function of rotor incidence. The figure illustrate that an efficiency of 80% was achieved at about 3.5°incidence.

In addition, the predictions of the turbine model are also evaluated at off-design conditions. Figure 7 show the mass flow rate as a function of total-to-static pressure ratio and rotational speed. The lines represent predicted mass flow rate, while the markers illustrate the experimental values. The figure show that the model predicts similar behaviour as the experimental case, but with certain differences. Most noticeable is the unphysical "bump" that occur as the pressure ratio approaches the critical value. It is observed that the bump is non-existent for isentropic flow, and becomes more significant as the efficiency decreases. Thus, it is likely that this behaviour is related to the way losses are predicted throughout the turbine. Furthermore, similar as for the design point comparison, the predicted choked mass flow rate exceed the experimental value slightly. The choked mass flow difference in percentage is approximately 1.12% and 2.61% at design rotational speed and 30% of design rotational speed, respectively. As expected the deviation is larger for off-design rotational speed. Moreover, it can be observed that the critical pressure ratio is slightly higher then experimental value (approximately 2.7 vs. 2.6).

Table 6: Operating conditions and comparison of performance parameters between the second experimental reference (Haas and Kofskey 1975) and model presented in this paper.

Variable	Haas and Kofskey 1975	Present work
Fluid	Air	-
$T_{0,\mathrm{in}}$	300 K	-
$p_{0,\mathrm{in}}$	8.27 bar	-
$p_{0,\mathrm{in}}/p_{\mathrm{out}}$	3.16	-
Ω	32 100 rpm	-
η_{tt}	83.2%	84.3%
$\dot{m}$	0.185 kg/s	0.184 kg/s
$\dot{W}$	11.73 kW	11.92 kW

4.3. Experimental case 2

The second experimental reference is the case presented in (Haas and Kofskey 1975). The operating conditions and performance parameters are shown in Table 6. Note that the efficiency here is the total-to-total efficiency. The results show that the efficiency is predicted well, with a deviation of 1.1 percentage points, while the predicted mass flow rate and work output differs from the experimental value by 0.66% and 1.56% respectively. The original report indicates that the stator throat area was fabricated 5.5% smaller than the design specification, which is accounted for in the simulations. Otherwise, the deviation in both mass flow rate and work output would exceed 4.5%.

4.4. Experimental case 3

Information on the third experimental turbine is presented in (Moffitt et al. 1980). This study presents a turbine operating at transonic conditions with relatively high specific work output. The experimental conditions and results are shown in Table 7. Note that the pressure ratio here is the total-to-total pressure ratio. The results show a deviation of 4.5 percentage points in efficiency, 3.36% in mass flow rate and 6.11% in work output. The results suggest that the model predicts performance of transonic turbines less

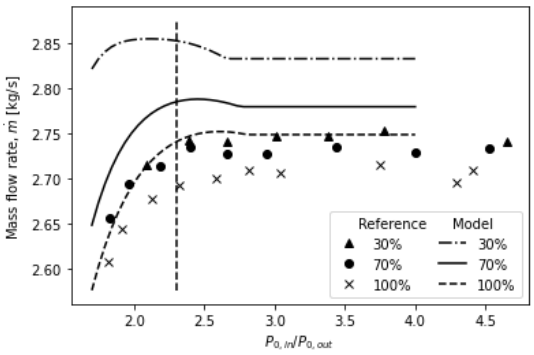

Figure 7: Mass flow rate as a function of total-to-static pressure ratio and percentage of design rotational speed. The lines represent predicted values, while the markers are the measured values for Experimental case 1. The vertical dashed line indicates the design pressure ratio.

Table 7: Operating conditions and comparison of performance parameters between the third experimental reference (Moffitt et al. 1980) and model presented in this paper.

Variable	Moffitt et al. 1980	Present work
Fluid	Air	-
$T_{0,\mathrm{in}}$	378 K	-
$p_{0,\mathrm{in}}$	24.13 bar	-
$p_{0,\mathrm{in}}/p_{0,\mathrm{out}}$	3.44	-
Ω	10 600.8 rpm	-
η_{tt}	88.6%	84.1%
$\dot{m}$	8.018 kg/s	7.748 kg/s
$\dot{W}$	799.33 kW	750.52 kW

Table 8: Case definition and results for the design case study. The results are compared to the reference design case described in (Agromayor and Nord 2019).

Variable	Agromayor and Nord 2019		Present work	
Fluid	R125		-	
$T_{0,\mathrm{in}}$	428.15 K		-	
$p_{0,\mathrm{in}}$	36.18 bar		-	
p_{out}	15.34 bar		-	
$\dot{m}$	11.90 kg/s		-	
η_{ts}	88.72%		89.56%	
Ω	34 738.2 rpm		28 647.9 rpm	
$\dot{W}$	227.76 kW		229.89 kW	
Row	Stator	Rotor	Stator	Rotor
r_{m}	4.04 cm		4.30 cm	
H	2.02 cm	2.02 cm	2.02 cm	2.02 cm
(H/c)	1.772	2.000	1.900	2.000
(s/c)	0.579	0.693	0.588	0.690
(t_{te}/o)	0.0479	0.0489	0.0500	0.0500
θ_{in}	-	-15.00°	-	-15.01°
θ_{out}	80.00°	-74.49°	80.00°	-74.44°
δ_{fl}	0°	0°	-8.83°	10.00°

accurately than subsonic turbines, which is consistent with the high uncertainty associated with the supersonic correction factor of the Kacker and Okapuu loss model.

5. Design case study

A design case study was conducted to showcase the design optimization method. The results obtained for this design exercise are compared to the design obtained with the method described in (Agromayor and Nord 2019). As mentioned, the mass flow rate is an input variable for reference model. Thus, the mass flow rate was here constrained to match the reference case and obtain comparable results. The rest of the bounds and constraints where set such that they also match for the two models. The fixed input variables, key performance parameters and geometry are presented in Table 8.

The results show that this model predicts a design with 0.84 percentage points higher efficiency, and a very similar geometry except for the flaring angle. Indeed, the proposed model predicts highest efficiency at -8.83°flaring of stator row, and 10°of rotor row, with $\pm$10°being the upper and lower bounds. The exact same constraint is applied for the reference case, while that model predicts highest efficiency at 0° flaring.

6. Summary and Discussions

In this paper a method for preliminary design and performance analysis of one-stage axial turbines have been presented. This method is intended to be the basis for a robust design optimization method that takes into account off-design operating conditions. Both the performance analysis and design optimization modes have been tested and compared against relevant data.

The validation section showed that the model performed variably for the different reference cases. As expected, the model predicted similar performance for the numerical case study, but deviated significantly in some of the experimental cases. It is likely that the assumption of zero incidence/deviation is violated, which could cause the error in predicted efficiency. Differences in fabricated turbine vs. design could also cause deviations in performance parameters. Moreover, the model error was also observed to be greater for transonic conditions compared to subsonic, which is explained by the high uncertainty of the supersonic correction factor of the Kacker and Okapuu loss model. In addition, unphysical behavior of the mass flow vs. pressure ratio curve was observed when the pressure ratio approached the critical value, which could cause the model to be less accurate. It is likely that this behaviour is a consequence of how the losses are calculated at the blade throats. As discussed previously, the loss coefficient is evaluated at the throat in the same way as the exit, while a strategy to split the losses could solve this problem.

The design case study resulted in a geometry similar to the reference case, with converging-diverging flaring angles being the most noticeable difference. This affect the flow area and hence the flow velocities, making the velocity higher at stator exit and lower at rotor exit compared to the reference case. The difference of flaring angle could arise as the reference case included a diffuser model at turbine exhaust, which recovers a fraction of the exit kinetic energy. Nevertheless, the preliminary design optimization method is confirmed to give similar results as comparable preliminary design tools.

7. Further work

To improve the accuracy of the model, it is suggested to do a comparative analysis of several loss models for axial turbines, and to account for incidence in the loss calculation. All loss models considered should be compared against experimental data, and a data collection should be conducted, either from available literature or experimental investigation. The data collection should also contain data from transonic/supersonic turbines to validate models in this flow regime. Only when this is conducted one can assess which loss model to use in this method.

In addition, the design method will be extended to account for off-design conditions. The objective function for this purpose will be extended to be a weighted average of efficiencies at several design points. The efficiencies could be weighted according to the occurrence of the corresponding conditions over an annual perspective.

Acknowledgment
The research leading to these results has received funding from the EEA Grants and the Technology Agency of the Czech Republic within the KAPPA Programme. Project code TO01000160.

References

Agromayor, Roberto and Lars O. Nord (2019). "Preliminary design and optimization of axial turbines accounting for diffuser performance". eng. In: *International journal of turbomachinery, propulsion and power* 4.3. Place: Basel Publisher: MDPI AG, p. 32. ISSN: 2504-186X.

Aissa, Mohamed Hassanine et al. (2019). "Optimisation of a turbine inlet guide vane by gradient-based and metamodel-assisted methods". eng. In: *International journal of computational fluid dynamics* 33.6-7. Place: Abingdon Publisher: Taylor & Francis, pp. 302–316. ISSN: 1061-8562.

Bell, Ian H et al. (2014). "Pure and Pseudo-pure Fluid Thermophysical Property Evaluation and the Open-Source Thermophysical Property Library CoolProp". eng. In: *Industrial & engineering chemistry research* 53.6. Place: WASHINGTON Publisher: American Chemical Society, pp. 2498–2508. ISSN: 0888-5885.

Bonaiuti, Duccio and Mehrdad Zangeneh (2009). "On the Coupling of Inverse Design and Optimization Techniques for the Multiobjective, Multipoint Design of Turbomachinery Blades". eng. In: *Journal of turbomachinery* 131.2. Place: NEW YORK Publisher: ASME, 21014–021014 (16). ISSN: 0889-504X.

Châtel, Arnaud, Tom Verstraete, and Grégory Coussement (2020). "Multipoint optimization of an axial turbine cascade using a hybrid algorithm". eng. In: *Journal of turbomachinery*. Publisher: ASME, pp. 1–15. ISSN: 0889-504X.

Colonna, Piero et al. (2015). "Organic Rankine Cycle Power Systems: From the Concept to Current Technology, Applications, and an Outlook to the Future". eng. In: *Journal of engineering for gas turbines and power* 137.10. Place: NEW YORK Publisher: ASME. ISSN: 0742-4795.

Denton, J.D (1993). "Loss mechanisms in turbomachines". eng. In: *Journal of turbomachinery* 115.4. Place: New York, NY Publisher: American Society of Mechanical Engineers, pp. 621–656. ISSN: 0889-504X.

Dixon, S.L. (2014). *Fluid mechanics and thermodynamics of turbomachinery*. eng. Edition: 7th ed. ISBN: 9780124159549 Place: Amsterdam.

Haas, J. E and M. G Kofskey (1975). *Cold-air performance of a 12.766-centimeter-tip-diameter axial-flow cooled turbine. 1: Design and performance of a solid blade configuration*. eng.

Jiménez-Arreola, Manuel et al. (2018). "Thermal power fluctuations in waste heat to power systems: An overview on the challenges and current solutions". eng. In: *Applied thermal engineering* 134. Place: OXFORD Publisher: Elsevier Ltd, pp. 576–584. ISSN: 1359-4311.

Kacker, S. C and U Okapuu (1982). "A Mean Line Prediction Method for Axial Flow Turbine Efficiency". eng. In: *Journal of engineering for gas turbines and power* 104. Publisher: ASME, pp. 111–119. ISSN: 0742-4795.

Macchi, Ennio and Marco Astolfi (2017). *Organic rankine cycle (ORC) power systems : technologies and applications*. eng. ISBN: 0-08-100511-3 Place: Amsterdam, Netherlands Series: Woodhead Publishing in energy ; Volume: Number 107.

Moffitt, T. P et al. (1980). *Design and cold-air test of single-stage uncooled turbine with high work output*. eng.

Moran, M.J. et al. (2015). *Principles of Engineering Thermodynamics*. Wiley. ISBN: 978-1-118-96088-2. URL: https://books.google.no/books?id=zfQwBgAAQBAJ.

Nusbaum, W. J and M. G Kofskey (1972). *Design and cold-air investigation of a turbine for a small low-cost turbofan engine*. eng.

Persico, G and M Pini (2017). "Fluid dynamic design of Organic Rankine Cycle turbines". eng. In: *Organic Rankine Cycle (ORC) Power Systems: Technologies and Applications*, pp. 253–297. ISBN: 978-0-08-100510-1.

Pini, M., G. Persico, and V. Dossena (June 2014). *Robust Adjoint-Based Shape Optimization of Supersonic Turbomachinery Cascades*. Vol. Volume 2B: Turbomachinery. Turbo Expo: Power for Land, Sea, and Air. DOI: 10.1115/GT2014-27064. URL: https://doi.org/10.1115/GT2014-27064.

Sanchez Torreguitart, Ismael, Tom Verstraete, and Lasse Mueller (2018). "CAD and Adjoint Based Multipoint Optimization of an Axial Turbine Profile". eng. In: *Evolutionary and Deterministic Methods for Design Optimization and Control With Applications to Industrial and Societal Problems*. Computational Methods in Applied Sciences. ISSN: 1871-3033. Cham: Springer International Publishing, pp. 35–46. ISBN: 978-3-319-89889-6.

Saravanamutto, H.I.H. et al. (2017). *Gas Turbine Theory*. eng. 7th. Harlow: Pearson Education Limited. ISBN: 978-1-292-09309-3.

Virtanen, Pauli et al. (2020). "Author Correction: SciPy 1.0: fundamental algorithms for scientific computing in Python". eng. In: *Nature methods* 17.3. Backup Publisher: SciPy 1.0 Contributors Place: United States Publisher: Nature Publishing Group, pp. 352–352. ISSN: 1548-7091.